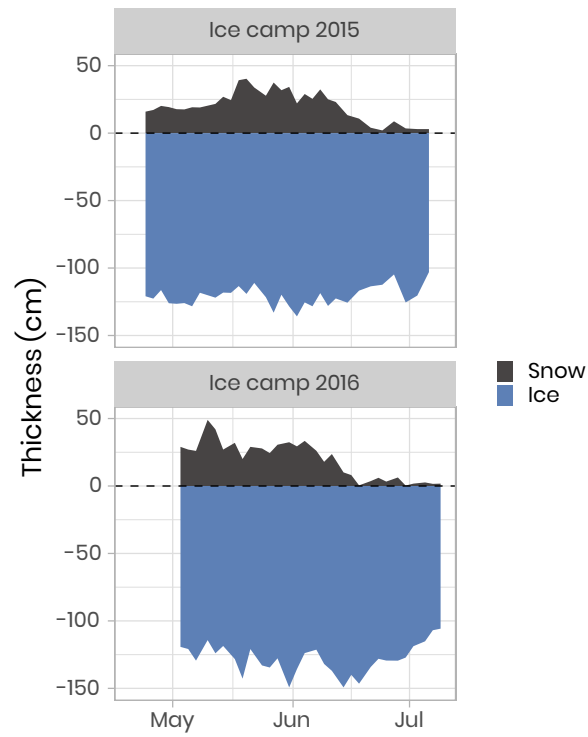


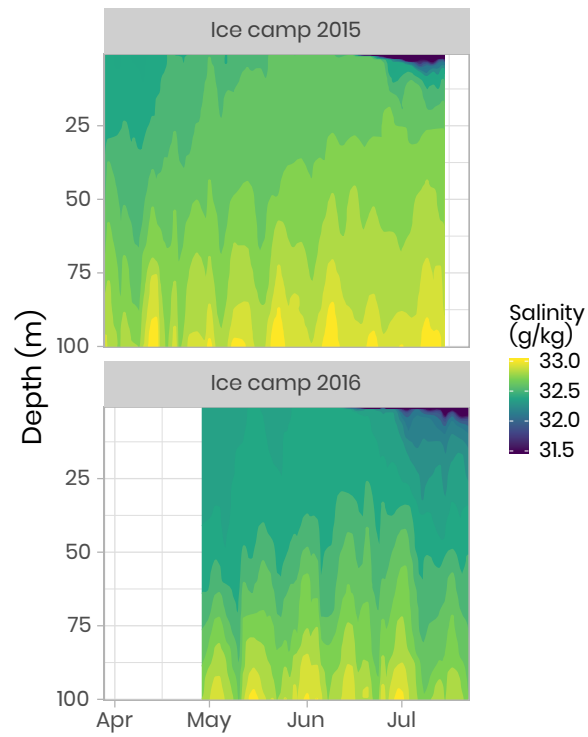
# Figures



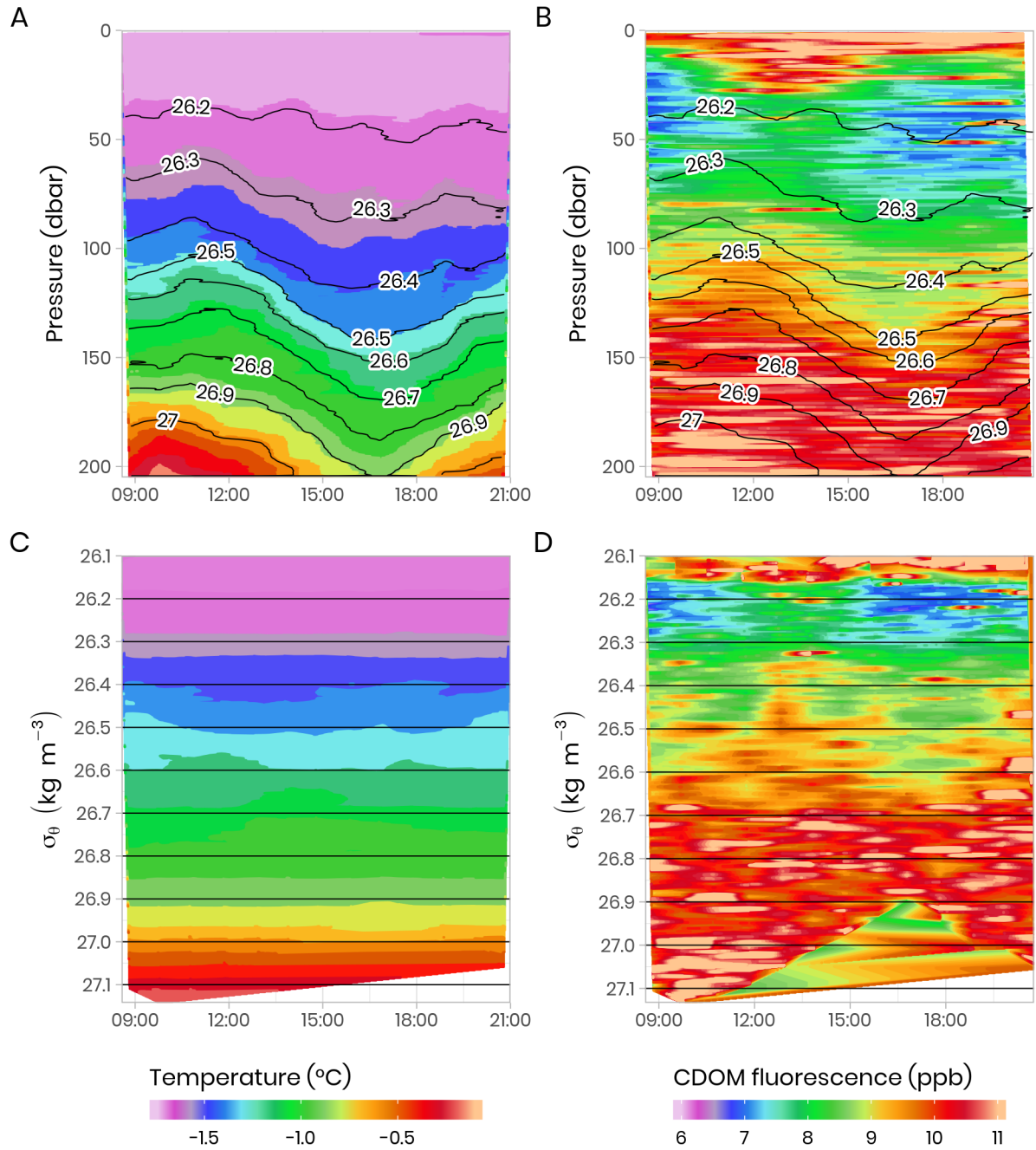
**Figure 1:** Location of the ice camp located near the Qikiqtarjuaq Island in the Baffin Bay. Projection used: EPSG-4326.



**Figure 2:** Temporal evolution of the snow and sea-ice thickness for both ice camp missions. The dashed horizontal line represents the snow/ice interface.



**Figure 3:** Temporal evolution of the salinity in the first 100 meters of the water column for both campaigns. Note that for visualization, salinity below  $31.5 \text{ g kg}^{-1}$  have been binned to  $31.5 \text{ g kg}^{-1}$ .



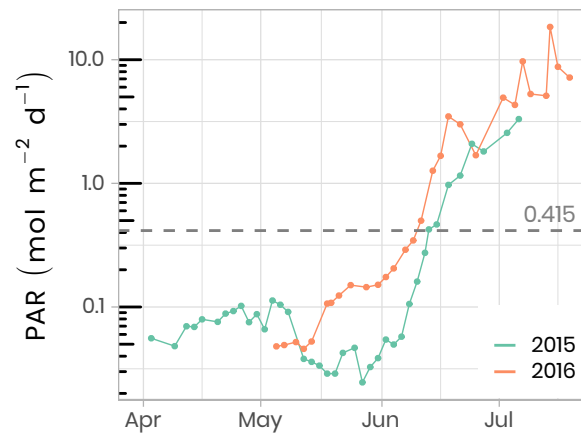


**Figure 5:** Temporal evolution of daily photosynthetically available radiation (PAR) at the sea-ice/water interface (1.3 m depth) for both ice camp missions. The horizontal dashed line shows the 0.415 mol photons  $\text{m}^{-2} \text{d}^{-1}$  threshold often used in the literature as the minimum light requirement for primary production.

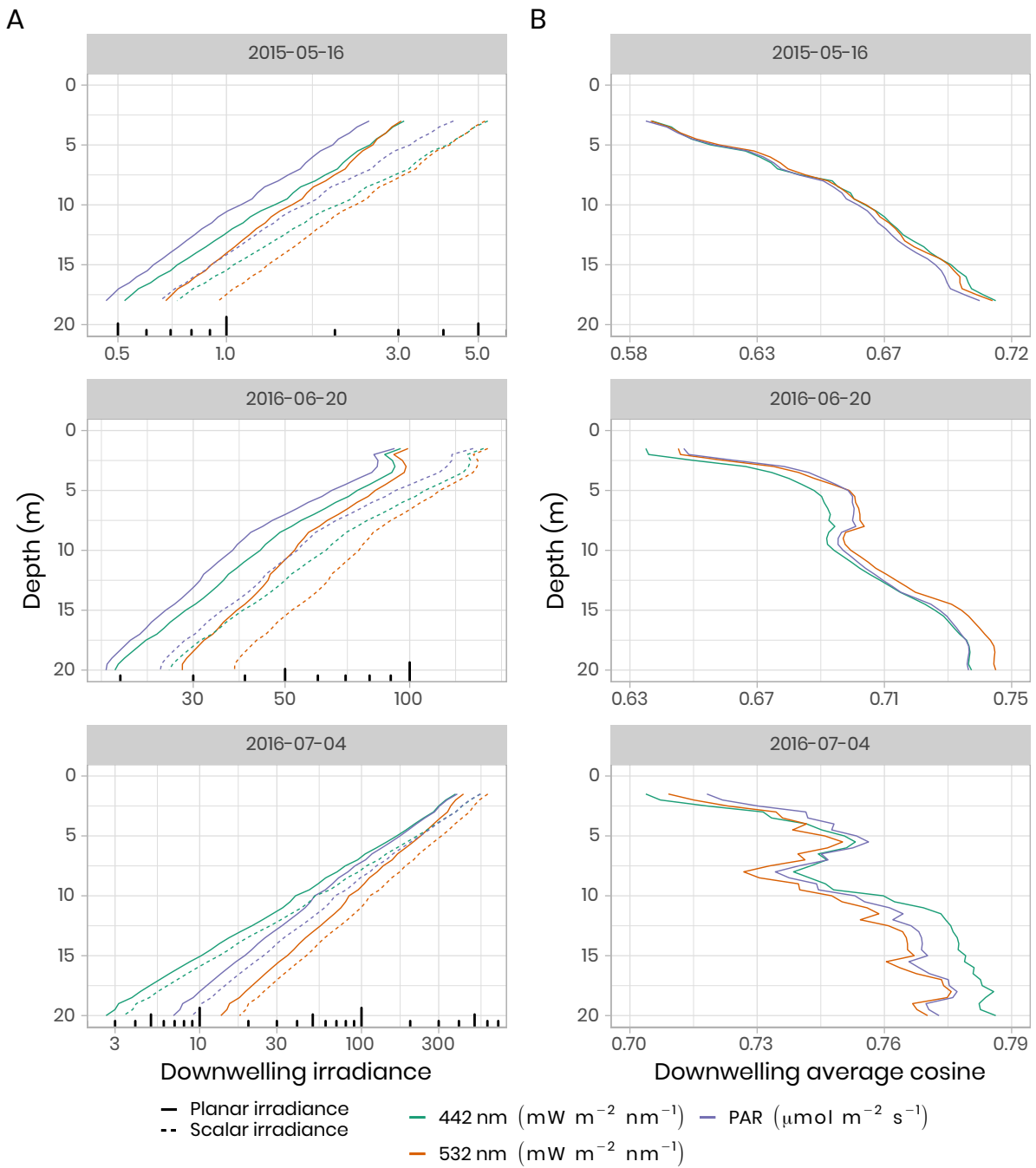


**Figure 6:** (A) Under-ice vertical profiles of downwelling planar and scalar irradiance at 442 nm, 532 nm and for PAR. (B) Calculated downwelling average cosine (unitless) was measured beneath snow-covered sea ice on 16 May 2015, beneath bare ice on 20 June 2016 and beneath a melt pond on 4 July 2016. Note the log scale for the irradiance measurements (A).

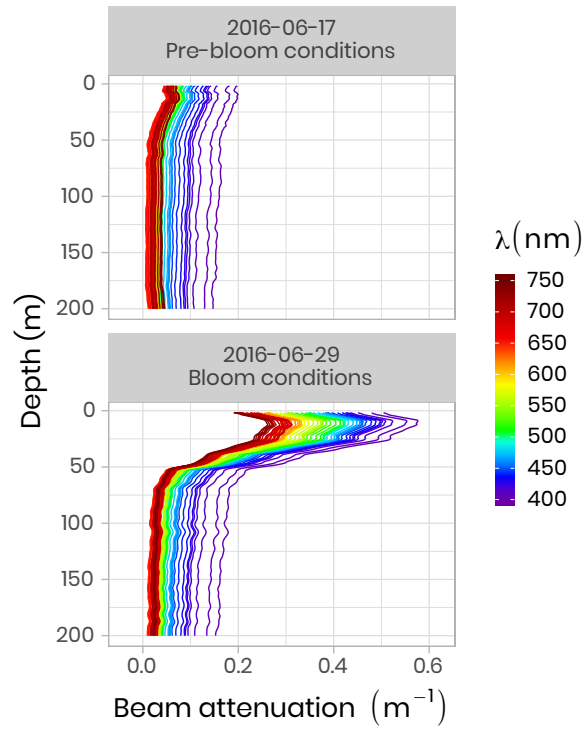


**Figure 7:** Beam attenuation coefficients ( $c$ ,  $\text{m}^{-1}$ ) measured in 2016 using an ACS before and during the phytoplankton bloom. Note that the colors of the lines correspond to wavelength frequencies.

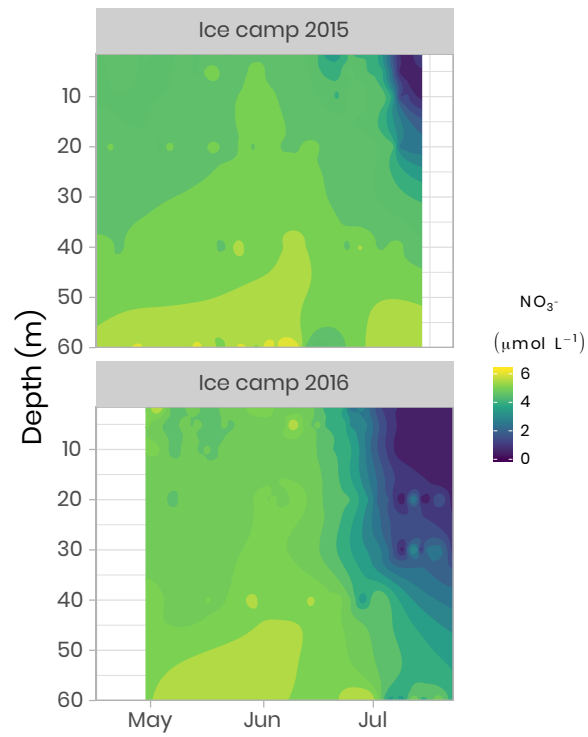


**Figure 8:** Temporal evolution of the nitrates in the first 60 m of the water column for both ice camp missions.



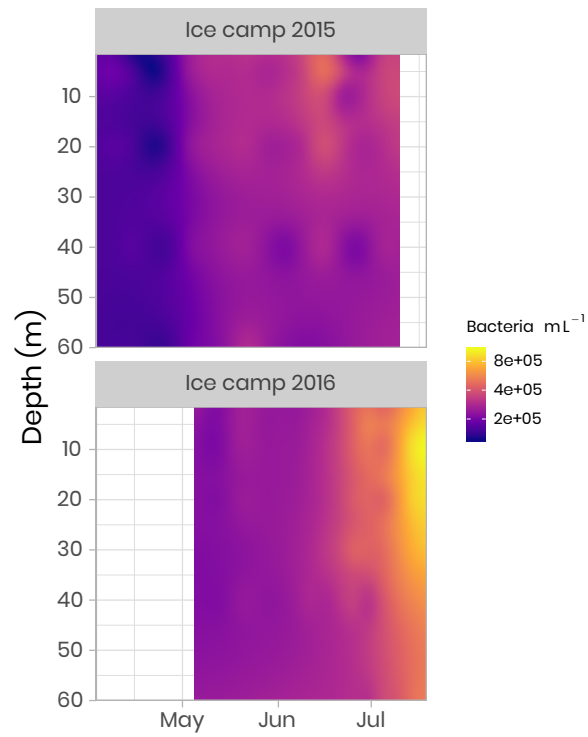


**Figure 9:** Concentration of bacteria in the water column at the ice camp in 2015 and 2016.

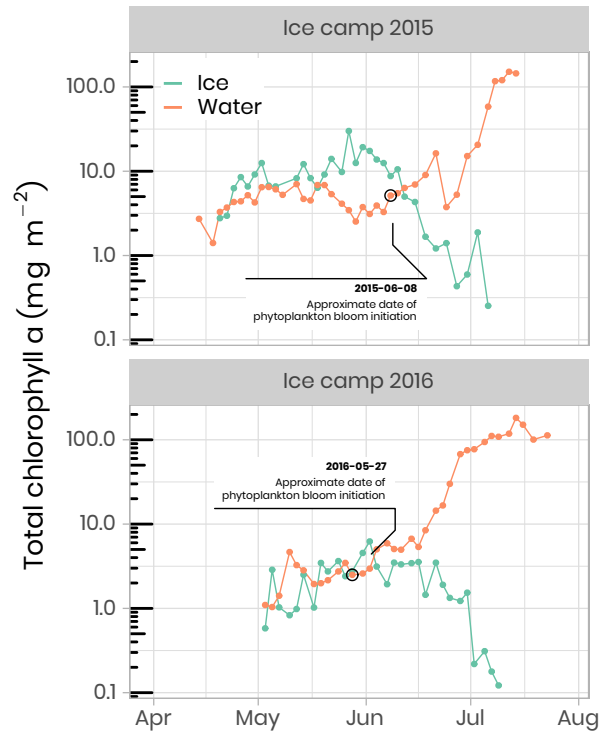


**Figure 10:** Temporal evolution of chlorophyll a in ice and water (depth-integrated) for both ice camp missions. Note that the water chlorophyll a have been integrated over the first 100 m of the water column whereas the ice chlorophyll a was measured on the bottom 0-10 cm of the ice cores. The details of the calculations to determine the approximate dates of phytoplankton bloom initiation can be found in Oziel et al. (2019).

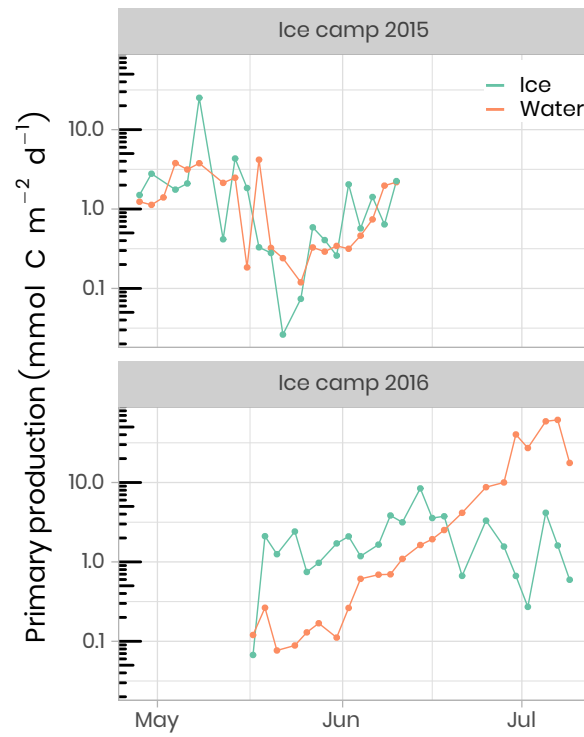


**Figure 11:** Temporal evolution of primary production a in ice and water (depth-integrated) for both ice camp missions.

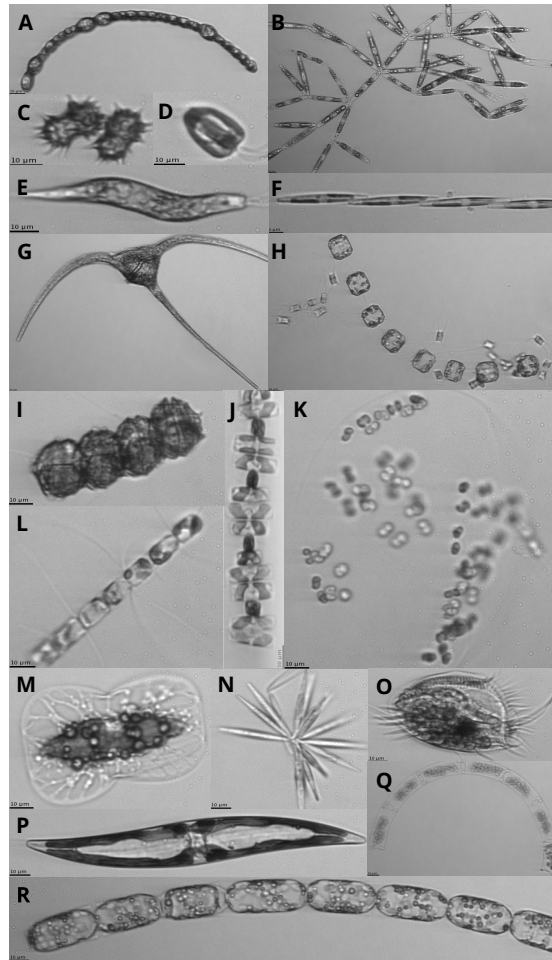


**Figure 12:** Images of protists sampled with the IFCB. Scale bar on images is 10 µm. Note that images are not to scale. (A) *Anabaena* sp. (B) *Nitzschia frigida* (C) *Polarella glacialis* (D) Flagellate (E) *Euglena* (F) *Pseudo-nitzschia* sp. (G) *Ceratium* sp. (H) *Thalassiosira nordenskiöldii* with *Attheya septentrionalis* (I) *Peridiniella catenata* (J) *Navicula pelagica* (K) *Phaeocystis* sp. colony (L) *Chaetoceros* sp. (M) *Entomoneis* sp. (N) *Synedropsis hyperborea* (O) Ciliate (P) Pennate diatom (Q) *Eucampia* sp. (R) *Melosira* sp.

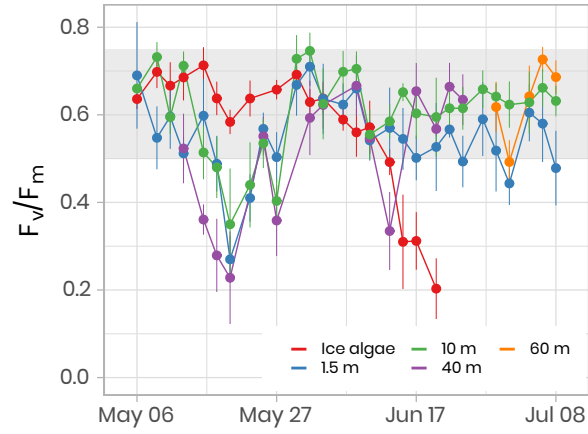


**Figure 13:** Temporal evolution of  $F_v/F_m$  for ice (last cm) and water underneath the ice (depths 1.5 m, 10 m, 40 m) samples for the ice camp 2016 between May 6<sup>th</sup> and July 8<sup>th</sup>.  $F_v/F_m$  monitoring on ice samples stopped on Day 172-June 20<sup>th</sup> because the Chl a fluorescence signal was not reliable anymore.  $F_v/F_m$  monitoring on 40 m and 60 m depth samples was limited between May 13<sup>th</sup> and June 24<sup>th</sup> and between June 29<sup>th</sup>-July 08<sup>th</sup>, respectively. The gray shaded area represents the range at which the algae are optimally growing.

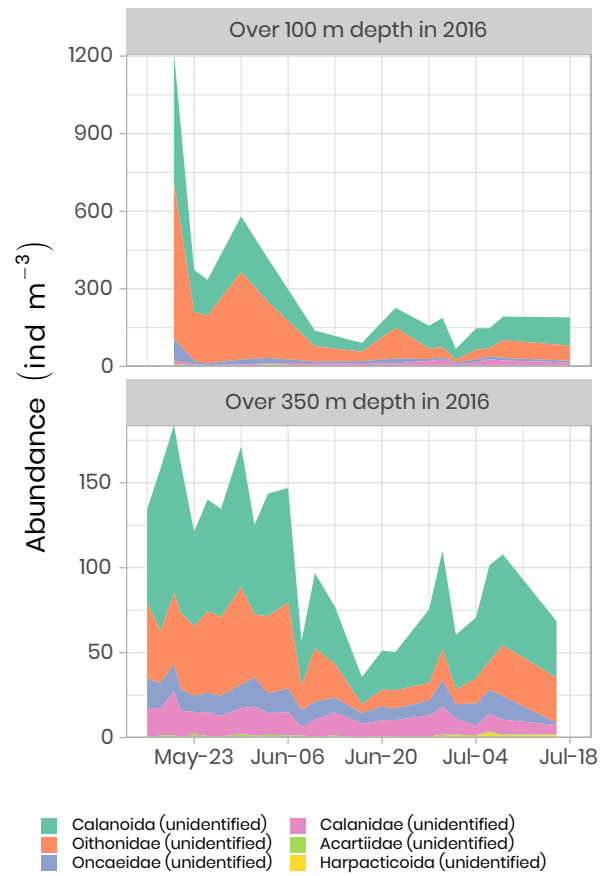


**Figure 14:** Time series of the abundance of the copepods (ind m<sup>-1</sup>) measured over the first 100 m and 350 m of the water column in 2016 using the zooscan. For visualization, only the six most abundant groups are presented in decreasing order of importance. Note the different y-axes in both panels.